International Journal of Mechanical Engineering and Technology (IJMET)
Volume 11, Issue 2, February 2020, pp. 56-72, Article ID: IJMET_11_02_006
Available online at http://www.iaeme.com/ijmet/issues.asp?JType=IJMET&VType=11&IType=2
ISSN Print: 0976-6340 and ISSN Online: 0976-6359

THE EFFECT OF DARRIEUS AND SAVONIUS WIND TURBINES POSITION ON THE PERFORMANCE OF THE HYBRID WIND TURBINE AT LOW WIND SPEED

Nawfal M. Ali, Dr. Abdul Hassan A. K and Dr. Sattar Aljabair
Department of Mechanical Engineering, University of Technology, Baghdad, Iraq

ABSTRACT

This paper presents an experimental and numerical simulation to investigate a hybrid vertical axis wind turbine model highly efficient which can be worked at low wind speed by studying the aerodynamic characteristics of four models of hybrid VAWTs. The hybrid WT consists of the SWT having two blades and the DWT type straight having two blades. Four models were constructed to study experimentally and numerically to choose the best model. Two models were DWT in the upper and SWT in the lower, also two models were SWT in the upper and DWT in the lower. The phase stage angle between the turbines is 0^o and 90^o. The experimental and numerical results showed that the performance of hybrid WT where DWT in the upper and SWT in the lower with phase stage 90^o is better than in the other models, it can be started to work at a wind velocity of 2.2 m/s. At the wind velocity 3 m/s, the values of the parameters are the rotational speed (198 rpm), the C_P (0.3195), the C_T (0.2003), the TSR (1.6) and self-starting rotation at this value of wind velocity (3 m/s). The efficiency of extracting the wind power by hybrid WT is (51.2 %).

Keywords: Hybrid wind turbine, Vertical axis wind turbine, Low wind speed.

Cite this Article: Nawfal M. Ali, Dr. Abdul Hassan A. K. and Dr. Sattar Aljabair, The Effect of Darrieus and Savonius Wind Turbines Position on the Performance of the Hybrid Wind Turbine at Low Wind Speed. *International Journal of Mechanical Engineering and Technology* 11(2), 2020, pp. 56-72.
http://www.iaeme.com/IJMET/issues.asp?JType=IJMET&VType=11&IType=2

NOMENCLATURE

A	Hybrid swept area (m^2)	P	Static pressure
As	Swept area of turbine (m^2)	T	Dynamic torque (N.m)
C_p	Power coefficient	Ta	Ambient temperature (K)
C_T	Torque coefficient	T_{or}	Torque (N.m)
c	Darrieus blade chord (mm)	TSR	Tip speed ratio
d	Savonius blade chord (mm)	w	Distance between turbines (mm)
D	Savonius rotor diameter (mm)	$\vec{u}$	Relative velocity of fluid
e	Shaft distance (mm)	DWT	Darrieus wind turbine
		HWT	Hybrid wind turbine

F	Force (N)	RANS	Reynolds Averaged Navier-Stokes
h	Savonius blade height (mm)	SST	Shear Stress Transport
H	Darrieus blade height (mm)	SWT	Savonius wind turbine
N	Rotational speed (rpm)	VAWT	Vertical axis wind turbine
R	Darrieus rotor radius (mm)	WT	Wind Turbine
Rg	Gas constant (287 J/kg.K)	$\vec{\Omega}$	Rotational speed (rpm)
$\vec{r}$	Position vector	μ	Viscosity (Pa.s)
rp	Radius of pulley (mm)	ρ	Air density (kg/m^3)
P_{atm}	Atmospheric pressure (Pa)	ω	Angular velocity (rad/s)
P_{AV}	Available power in the wind (W)	Sui	Centrifugal and Coriolis force
P_T	Power produced from turbine (W)	τij	Average shear stress

1. INTRODUCTION:

In recent years, the wind energy has become one of the most economical renewable energy technologies. Today, electricity-generating wind turbines employ proven and tested technology and provide a secure and sustainable energy supply. At good, windy sites, the wind energy can already successfully compete with conventional energy production. Many countries have considerable wind resources, which are still untapped. So, the wind energy has to compete with many other energy sources in the future. To compete with others, it had to cope with the least affirmative conditions to maximum positive conditions. The usual challenge for the wind turbine is performing at low wind speed [1].

A hybrid vertical axis wind turbine (HVAWT) is designed by the combination of two types of vertical turbine Darrieus and Savonius (on a common shaft) that can work in sites having low wind velocity. The benefits of this design are starting at low wind speeds and obtain a good efficiency. This model can be used to the wind power available on the highways caused by the movement of the vehicles. [2] studied the characteristics of the parameters by numerical simulation for a hybrid wind turbine (3 blades Savonius and 3 blades Darrieus) with various overlap conditions and compared with previous experimental results. The results showed that the maximum C_P (0.377) is at an overlap ratio of 20%, maximum C_T (1.271) at an overlap ratio of 30% and maximum TSR (0.414) at an overlap ratio of 16.2%. [3] investigated the parameters of a combined VAWT, including dynamic torque, starting torque coefficients and power performance that was simulated and analyzed. DWT is straight-bladed and airfoil type NACA0012 the number of blades is 4, SWT with 2 buckets. The results showed that the power produces at all TSRs, that means the power performance for the combined VAWT improved at a low rotational speed field. The dynamic torque performance increased at the low TSR. [4] studied the performance of a hybrid VAWT by experimental work procedure. DWT H-type with three blades and airfoil was DU06W200 combined with an SWT that has two conventional buckets. The results depicted that the combining between Darrieus and Savonius WT makes an efficient hybrid WT, it has improved the self-starting with a higher power coefficient. [5] investigated aerodynamics and the starting performance for a hybrid VAWT with the assistance of CFD simulations. Hybrid VAWT consists of DWT H-type with 3 blades and airfoil NACA0021, SWT with 3 blades and different distances between blade and center of rotation (d = 0, 50, 100, 150) mm, the wind velocity is 9 m/s. The results showed that the C_P of the hybrid VAWT decreases when increasing the distance, while the starting torque can be improved. The position of the Savonius blade for the installation is very important. [6] studied the design of hybrid VAWT that can be started at low wind speed (4.8 m/s) and obtained a good efficiency. The results showed that the efficiency of hybrid VAWT reached up to 37% at a TSR of 0.9 and with no overlap. When increasing TSR, the C_P and overall efficiency increase. TSR and C_P decrease when the wind velocity increases. The effect of geometrical and operational parameters (C_P), (C_{TS}) and (C_T) on the performance of hybrid WT was studied by [7]. Four models of HWT were taken to experimental tests. Wind velocity range in experimental tests was from (0-12) m/s. The results showed that the turbine power of the model (3 blades Savonius with 3 blades Darrieus) is very good at wind velocity range 2-8 m/s compared with the other models, also the C_P for this model is 0.23. [8] studied the evaluation of the optimal design of Darrieus vertical axis wind turbine by CFD analysis and experimental tests, through analyzing six models of Darrieus wind turbines, number of blades and tip speed ratio. The airfoil profile used in the turbine blades was DU06W200 and constant geometry dimensions to turbines. The types of six models of DWT were straight, twisted 70^o and helical 120^o, all types with two and three blades. The results showed that Darrieus WTs straight types can be self-started at the wind velocity 3 m/s, but the twisted types started over 5 m/s and the helical types started over 6 m/s. The performance of Darrieus WT with 2 blades rotor is better than the other models. At low wind velocity (3 m/s) the value of C_P is (0.2495), the C_T (0.174), the rotational speed (198 rpm) and can be self-started at this wind velocity. The efficiency of extracting the wind power by Darrieus WT is (39 %). [9] used Savonius WT with semi-circular profile blades and single-stage having a various numbers of blade (two, three and four). The fourth model has two blades with two stages, the phase angle between stages one and two is 90^o. The overlap distance is zero for all models. The experimental and numerical results showed that the performance of Savonius WT having two blades is better than the other models at low wind speed. The maximum experimental C_P and C_T for two blades rotor are 0.23 at TSR 0.685 and 0.402 at TSR 0.175, respectively. The efficiency of extracting the wind power by Savonius WT is (38.81 %).

In this study, a comparison was execute between four models of hybrid wind turbine to study the behavior and performance of these models at wind speed range (3-7.65) m/s, especially at (3 m/s) with different tip speed ratios. Experiments and numerical analyses were carried out to choose the best model that can be worked at the low wind velocity conditions (3 m/s).

2. HYBRID WIND TURBINE (HWT) PERFORMANCE

The performance of Hybrid VAWTs is explained by (C_T), (C_P), (λ) given by [3,7]. Figure (1) shows the geometry and dimensions of the hybrid wind turbine:

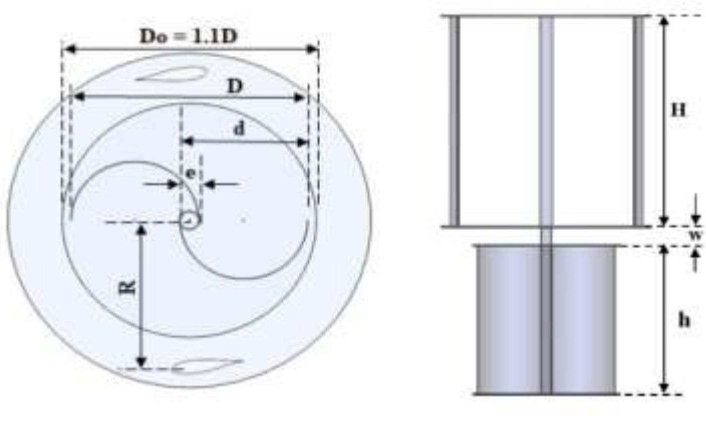

Figure 1 The geometry and dimensions of the hybrid wind turbine

The swept area for HWT (A) is

$$A = \sum(A_{s\ Darrieus} + A_{s\ Savonius}) = 2RH + Dh \quad (1.1)$$

$$\lambda = \frac{\omega R}{u} \quad (1.2)$$

$$C_T = \frac{T}{0.5\ \rho A u^2 R} \qquad (1.3)$$

$$C_P = \frac{P_{Turbine}}{P_{Available}} = \frac{T\ \omega}{0.5\ \rho A u^3} = \frac{T}{0.5\ \rho A u^2 R}\ \frac{R\omega}{u} = C_T\ .\ \lambda \qquad (1.4)$$

In this study, four models are taken to study and make a comparison between them to find out the best model of HWT, the study condition is at low wind velocity (3 m/s).

3. HYBRID WIND TURBINE MODELS

The four models of experiments tests are named as the following, the dimensions of HWTs are listed in the table (1).

- Case 1 represented the hybrid WT that consists of Darrieus WT upper and Savonius WT lower with phase stage 90^o. Figure (2-a) shows the geometry of Case 1.
- Case 2 represented the hybrid WT that consists of Darrieus WT upper and Savonius WT lower with phase stage 0^o. Figure (2-b) depicts the geometry of Case 2.
- Case 3 represented the hybrid WT that consists of Savonius WT upper and Darrieus lower with phase stage 90^o. Figure (3-a) shows the geometry of Case 3.
- Case 4 represented the hybrid WT that consists of Savonius WT upper and Darrieus lower with phase stage 0^o. Figure (3-b) reveals the geometry of Case 4.

Table 1: The dimensions of hybrid WTs (all Cases)

Number of blades	D (mm)	d (mm)	h (mm)	R (mm)	c (mm)	e (mm)	w (mm)
2-Savonius 2-Darrieus	350	175	380	250	100	25	70

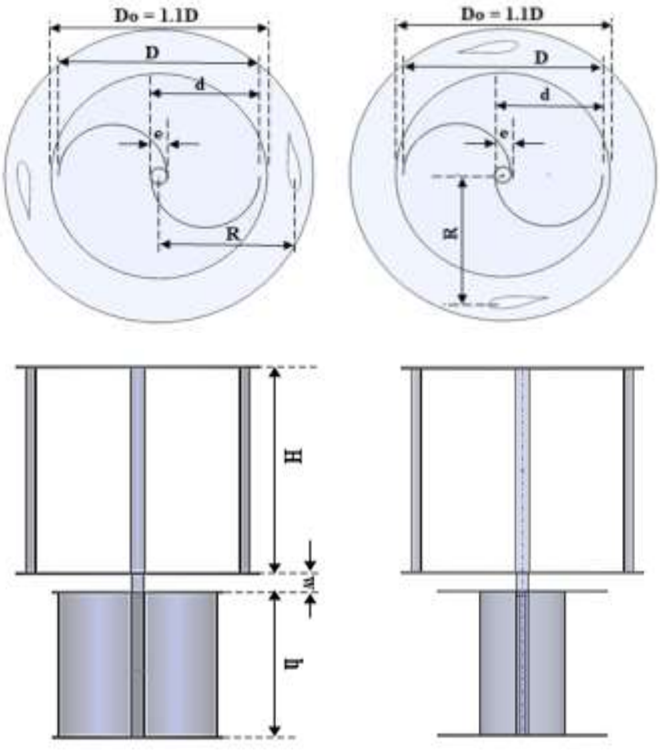

(a) **(b)**

Figure 2 Hybrid WT type Darrieus (upper) and Savonius (lower) model: (a) phase angle 0^o and (b) phase angle 90^o .

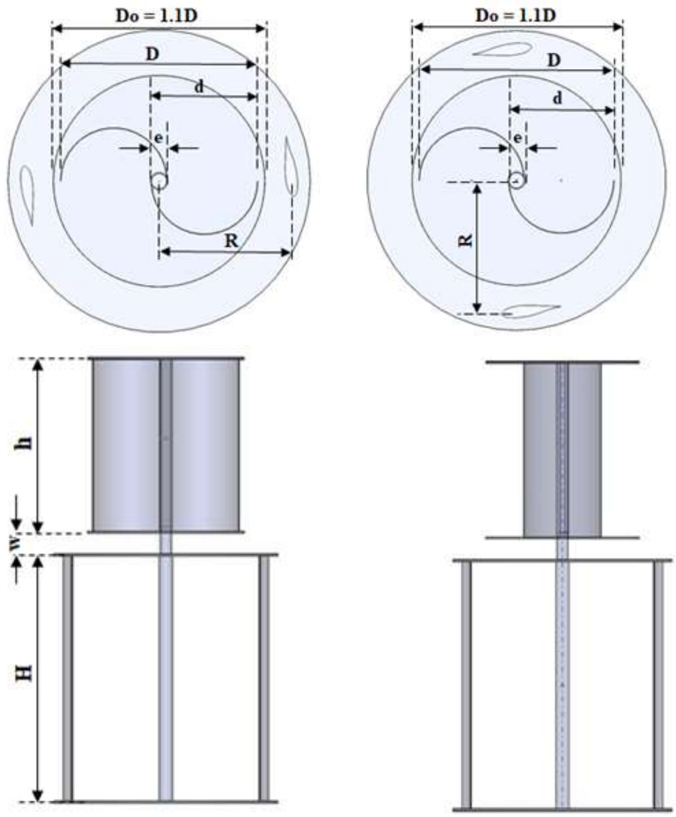

(**a**) (**b**)

Figure 3 Hybrid WT type Savonius (upper) and Darrieus (lower) model: (a) phase angle 0^o and (b) phase angle 90^o

4. THE EXPERIMENTAL WORK

4.1. Experimental Setup

Experiments were conducted using a subsonic wind tunnel under an open type test section, shown in fig. (4 - a,b,c) with the test section containing the turbine model and the measurement devices assembly with a cross-section of frontal view of 1m x 1.25m. Double butterfly valve was used to control and regulate the airflow rate, and the airspeed range was (0 - 9) m/s. The turbine models were fixed at 250 mm between the rotor shaft and exit of the wind tunnel. Digital tachometer used to measure the rotational speed of the wind turbine. Digital force gauge was utilized to measure the force (F) produced from the rotor shaft, the torque can be calculated by:

$$T_{or} = F \times r_p \qquad (1.5)$$

Where, the radius of pulley (r_p) = 50 mm.

The static pitot tube was used to measure the airflow speed in the wind tunnel, it was connected with a macroscopic manometer. The digital thermometer was utilized to measure the ambient temperature. The pressure gauge was used to measure atmospheric pressure. The air density is given by:

$$\rho = \frac{Patm}{Ta \times Rg} \qquad (1.6)$$

Figure 4-a A subsonic wind tunnel

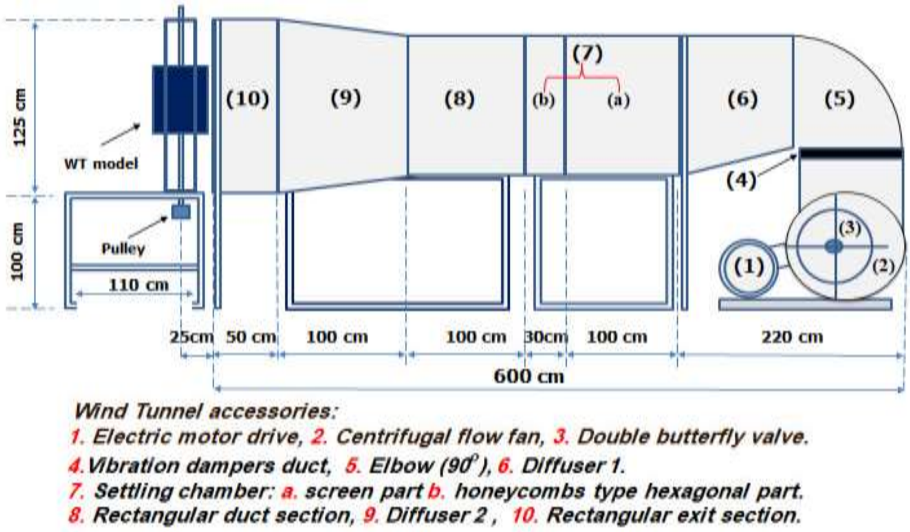

Figure 4-b: Schematic diagram for wind tunnel with the dimensions details

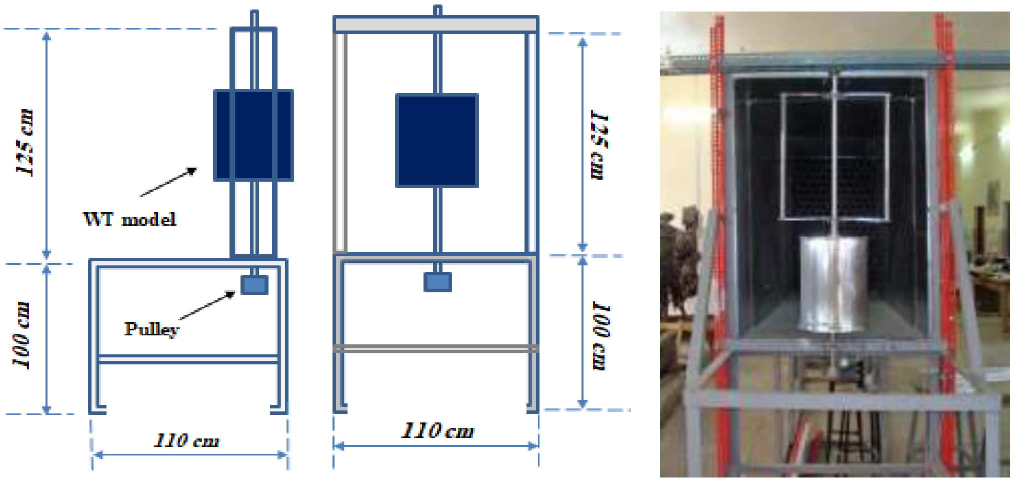

Figure 4-c: The test section rigs with the turbine model and dimensions details

5. NUMERICAL MODEL

To obtain a successful design and suitable geometry for the VAWT rotor, modeling styles should be applied. ANSYS-CFX software was used in this study for simulation and validation. The results were compared with experimental and numerical data, and the error was assessed. Transient conditions were considered for these modeling. Figure (5-a) shows the 3D computational domain for the turbine rotor model. Two parts are separated by a sliding interface in the domain. Wind tunnel testing zone represents the stationary, that is the first part of the domain. The dimensions of the wind tunnel (stationary domain) are 4 m x 4 m x 8 m. Figure (5-b) displays the mesh on the rotating domain, the mesh on the rotor and the mesh on the endplate in the rotor, also it appears the mesh near the blade showing the boundary layers. The flow around the rotor is turbulent, thus the simulation of CFD around the rotor is complex. Simulations of CFD were applied to solve the cases based on 3D steady finite volume incompressible Reynolds Averaged Navier-Stokes (RANS) equations. Controlling the equations of turbulence flow are continuity and Navier - Stokes equations, these equations in conservative forms are [10,11]:

$$\frac{\partial ui}{\partial x_j} = 0 \quad (1.7)$$

$$\frac{\partial}{\partial x_j}\left(\rho\overline{u_i u_j}\right) = \frac{-\partial\overline{P}}{\partial x_i} + \frac{\partial}{\partial x_j}\left(\overline{\tau_{ij}} - \rho\overline{\acute{u}_i \acute{u}_j}\right) + S_{ui} \quad (1.8)$$

Where:

$$S_{ui} = -\rho\,[2\,\vec{\Omega} \times \vec{u} + \vec{\Omega} \times (\vec{\Omega} \times \vec{r}\,)] \quad (1.9)$$

$$\overline{\tau_{ij}} = -\mu\left(\frac{\partial\overline{u_i}}{\partial x_j} + \frac{\partial\overline{u_j}}{\partial x_i}\right) \quad (1.10)$$

To solve the case of the flow field around the rotor numerically, the turbulence models were added in RANS CFD solvers. The best model is that gives accepted results and agreement with the experimental results.

5.1. Boundary Conditions

The boundary conditions in simulations of this study are:

- Wind velocity at the entrance stationary domain is 3 m/s, and distance from the axis of the rotational domain is 1.5 m.
- The pressure in the outer face is equal to the atmospheric pressure.
- The blade of the rotor is set as a non-slip smooth wall. To obtain good results and more strictly study the flow in the boundary layers of rotor blade in this study, a prismatic mesh was applied on the sides of rotor blades to obtain correctly the boundary layer. Accordingly, the density of meshes was higher near the wall of rotor blades than the other parts.
- The walls (sides and top) of the stationary domain are set as opening to the atmospheric pressure.
- The base of the stationary domain is set as a non-slip smooth wall.
- The SST k-ω turbulence model is applied in numerical simulation.

5.2. Turbulence Models

The precedent studies used a 3D SST k-ω turbulence model which agrees with the experimental work of [12,13,14]. This model employs to analyze the transient forces that affect DWTs. The advanced turbulence models used in this work need a very fine mesh near the wall so that Y+ < 5 [15,16], to get a good result. So in this study, the SST k-ω turbulence model was applied in numerical simulation.

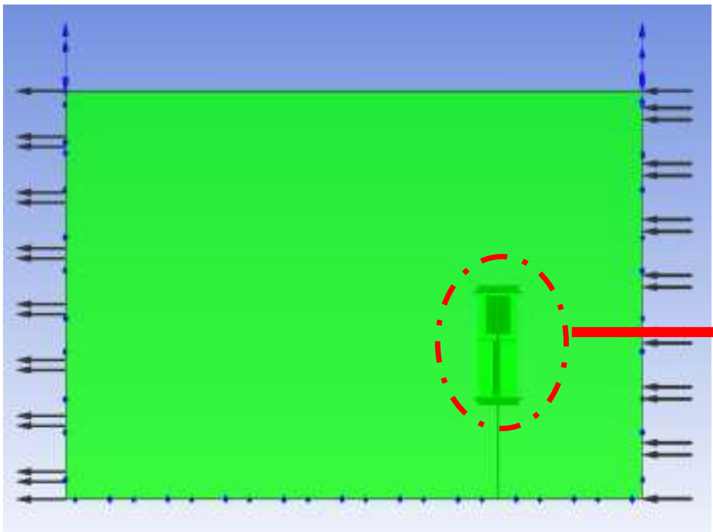

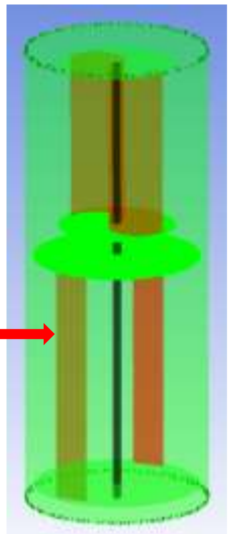

Figure 5-a : The 3D computational domain for the stator and turbine rotor.

Figure 5-b: The mesh of rotating domain

6. RESULTS AND DISCUSSION

The effect of model types and phase angle between the turbines is shown in Figs. (6.1) to (6.9). The power coefficient (C_P) value increases with the increase of TSR value for all cases at constant wind velocity (3 m/s) for experimental results. Figure (6.1) illustrates the relationship between the C_P of the HWT cases with various values of TSR for the experimental results at wind velocity (3 m/s), the C_P for case 1 is higher than other cases at TSR more than 1.4. The relation between C_P and wind velocity (u) is evinced in Fig. (6.2), the C_P values increases with increasing (u) value for all cases, and it is noted that the cases 1 and 2 can be worked at wind velocity 2.2 m/s (self-starting). The C_P value of case 1 is higher than case 2 for all (u) values. Figure (6.3-a and b) shows a comparison of the relation C_P - TSR at constant wind velocity (3 m/s) between the experimental and numerical results for cases 1 and 3, respectively, the values of C_P for experimental and numerical results are convergent values. Table (2) lists the experimental results of the (C_P) at various wind velocities for HWT cases, from the table, it is noted that cases 1 and 2 can be worked self-starting at wind velocity 2.2 m/s and this is the improvement on HWT.

Table 2 The C_P at various wind velocity for HWT cases

HWT cases	**Wind velocity (m/s)**						
	2.2	**3**	**4**	**4.5**	**5.15**	**6.45**	**7.65**
1	0.1965	0.3195	0.3243	0.3392	0.3442	0.3691	0.3897
2	0.1001	0.2440	0.2489	0.2530	0.3217	0.3541	0.3649
3	----	0.3242	0.3336	0.3436	0.3482	0.3681	0.3886
4	----	0.2672	0.2709	0.2768	0.3051	0.3379	0.3679

The torque coefficient (C_T) value at the experimental results increases with increasing the TSR value for all cases at constant wind velocity (3 m/s). Figure (6.4-a) manifests a comparison of the relation C_T - TSR at constant wind velocity (3 m/s) between the HWT cases for the experimental results. Figure (6.4-b) shows a comparison of the relation C_T with various wind velocities between the HWT cases for the experimental results, the value of the C_T increases to a certain extent, then the value decreases and increases again for all cases. Figure (6.5-a and b) elucidates a comparison of the relation C_T - TSR at constant wind velocity (3 m/s) between the experimental and numerical results for cases 1 and 3 respectively, the values of C_T for experimental and numerical results are convergent values. Table (3) lists the experimental results of the (C_T) at various wind velocities for HWT cases, also cases 1 and 2 can be worked at wind velocity 2.2 m/s.

Table 3 The C_T at various wind velocities for HWT cases

HWT cases	Wind velocity (m/s)						
	2.2	**3**	**4**	**4.5**	**5.15**	**6.45**	**7.65**
1	0.1665	0.2003	0.2003	0.1923	0.1888	0.1947	0.2043
2	0.1329	0.1772	0.1778	0.1746	0.1835	0.1945	0.2015
3	----	0.1885	0.2136	0.1884	0.1835	0.1921	0.2114
4	----	0.1675	0.1773	0.1543	0.1630	0.1783	0.2021

The value of C_T for case 1 is higher than in other cases for experimental results at wind velocity (3 m/s).

Performance parameters in terms of (C_P, C_T) for hybrid WT case 1 are shown in Fig. (6.6-a and b) related to TSR for the experimental and numerical results. Figure (6.6-a) shows the experimental results, both C_T and C_P values increase with the increase of TSR value. Figure (6.6-b) demonstrates the numerical results, both C_T and C_P values increase with increasing the TSR value to a certain value and then they decrease with increasing the TSR. Figure (6.7-a) represents the relationship between the rotational speed (N) and wind speed (u) for the HWT cases, it is noted that HWT cases 1 and 2 can be worked at the wind speed 2.2 m/s. The rotational speed (N) increases with the wind speed (u) increase for all cases. Figure (6.7-b) shows a comparison of the relation N - TSR at constant wind velocity (3 m/s) between the experimental and numerical results for cases 1, the values of N for the experimental and numerical results are convergent. Table (4) lists the experimental results of the (N) at various wind velocities for HWT cases.

Table 4 The rotational speed (N) at various wind velocities (u)

HWT cases	Wind velocity (m/s)						
	2.2	**3**	**4**	**4.5**	**5.15**	**6.45**	**7.65**
1	102	198	249	305	375	485	575
2	65	168	215	250	360	465	545
3	----	210	240	315	390	490	550
4	----	195	235	310	385	485	545

The rotational speed (N) is in (rpm).

The HWT case 1 and 2 can be worked at a wind velocity of 2.2 m/s, but case 1 has better performance than case 2. Figure (6.8-a) shows a comparison of the relation C_P - TSR at constant wind velocity (2.2 m/s) between the experimental and numerical results for case 1, the values of C_P for experimental and numerical results are convergent. Figure (6.8-b) depicts a comparison of the relation C_T - TSR at constant wind velocity (2.2 m/s) between the experimental and numerical results for case 1.

Performance parameters in terms of (C_P, C_T) for hybrid WT case 1 are shown in Fig. (6.9-a and b) related to TSR for the experimental and numerical results at constant wind velocity 2.2 m/s. Figure (6.9-a) shows the experimental results, both C_T and C_P values increase with the increase of TSR value. Figure (6.9-b) exhibits the numerical results, both C_T and C_P values increase with increasing the TSR value.

From the results in the tables (2, 3 and 4), it is shown that the performance of HWT (case 1) is better than in other cases, it can be started to work at the wind velocity of 2.2 m/s. When the wind velocity is 3 m/s, the values of the parameters for HWT case 1 are the rotational speed (198 rpm), the C_P (0.3195), the C_T (0.2003), the TSR (1.6) and self-starting rotation at this value of wind velocity (3 m/s). The values of the parameters for HWT case 1 at wind velocity 2.2 m/s are the rotational speed (102 rpm), the C_P (0.1965), the C_T (0.1665), the TSR (1.18) and self-starting rotation at this value of wind velocity (2.2 m/s). The efficiency of extracting the wind power by HWT is **51.2 %**.

7. CONCLUSIONS

The present study showed experimentally and numerically the effect of the combination between the two types of wind turbines (Savonius and Darrieus). The main conclusions from the results are as the following:

- The C_P and C_T values increase with increasing the TSR value for all cases at constant wind velocity (3 m/s) for the experimental results.
- The C_P values increase with increasing (u) value for all cases, case 1 and 2 (Darrieus at the upper and Savonius at the lower part with phase stage 90^o and 0^o, respectively) can be worked at wind velocity 2.2 m/s (self-starting).
- From the comparison of the relation C_T with various wind velocities between the HWT cases for the experimental results, the value of the C_T increases to a certain extent, then the value decreases and increases again for all cases.
- The value of C_T for case 1 is higher than in other cases for the experimental results at wind velocity (3 m/s).
- The performance of the hybrid WT case (1) is better than the other cases. At low wind velocity (3 m/s), the value of C_P is (0.3195), the C_T (0.2003), the rotational speed (198 rpm) and can be self-started at wind velocity 2.2 m/s.
- The efficiency of extracting the wind power for the Hybrid WT case (1) is 51.2 %.

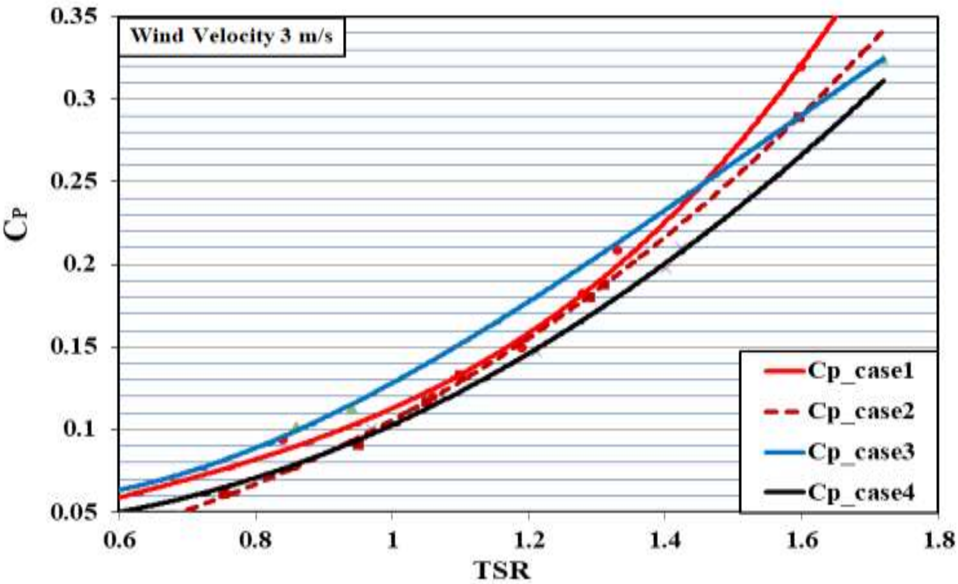

Figure 6.1: Experimental relation between C_P and TSR for all cases at a wind velocity of 3 m/s

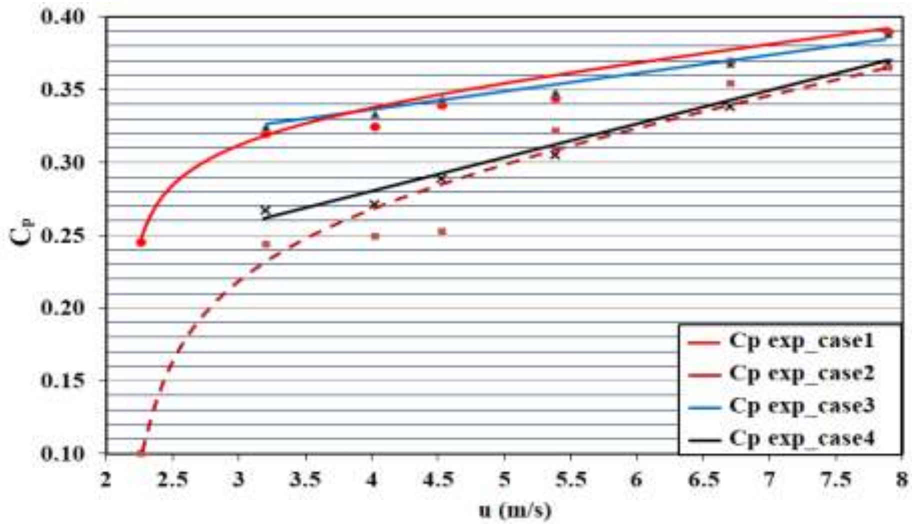

Figure 6.2: Experimental relation between Cp and u for all cases at various wind velocities

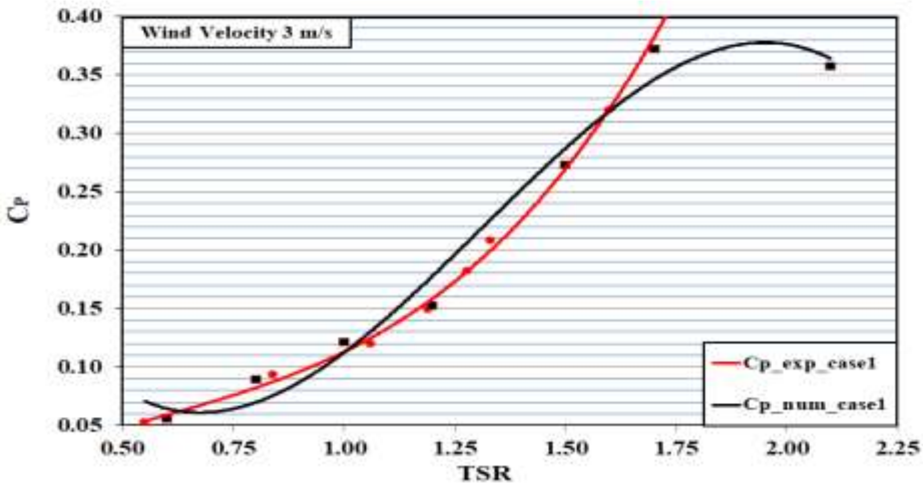

Figure 6.3-a: A comparison between experimental and numerical results for Case 1

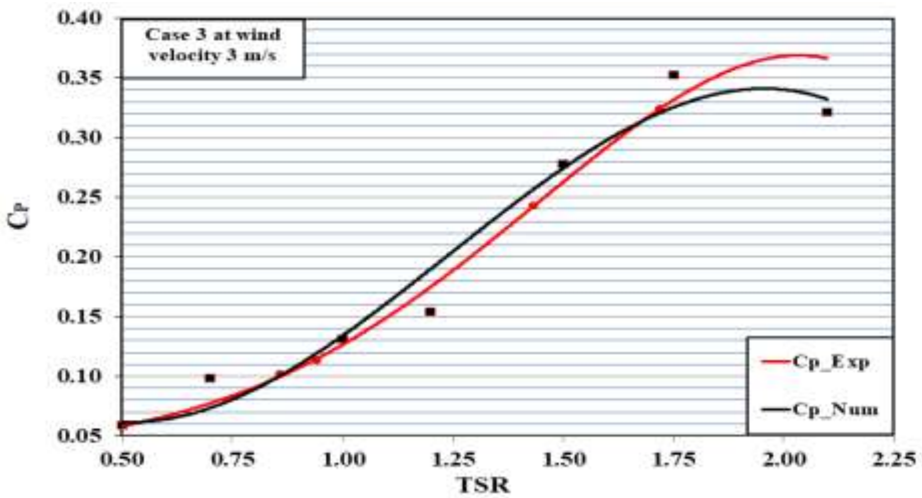

Figure 6.3-b: A comparison between experimental and numerical results for Case 3

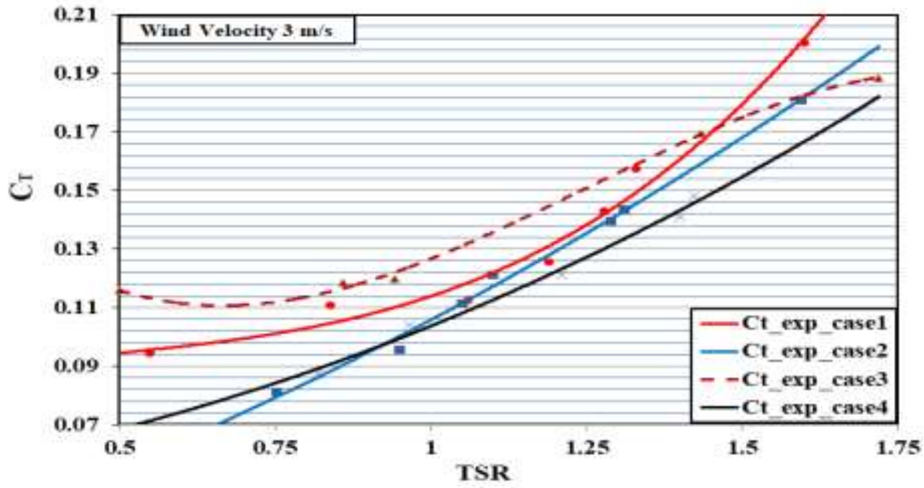

Figure 6.4-a: Experimental relation between CT and TSR for all cases at wind velocity 3 m/s

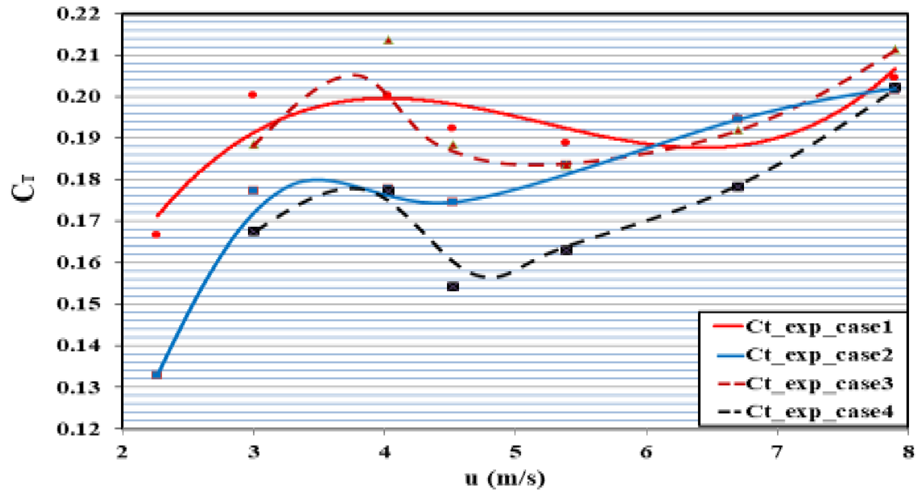

Figure 6.4-b: Experimental relation between CT and TSR for all cases at various wind velocities

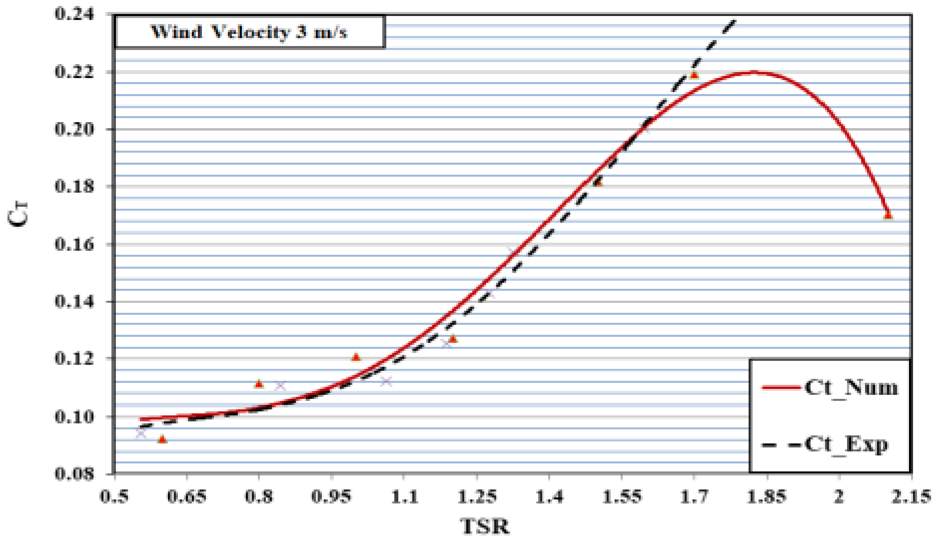

Figure 6.5-a: A comparison (CT) between experimental and numerical results for Case 1

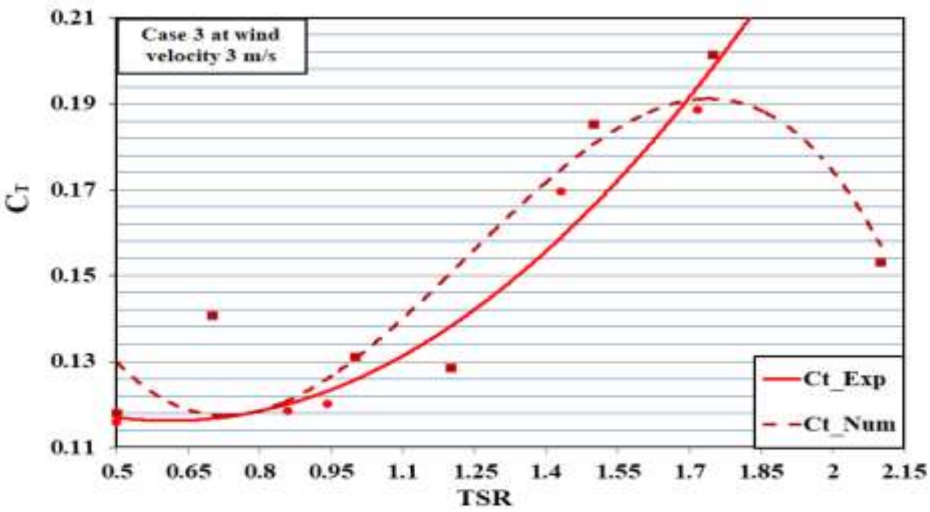

Figure 6.5-b: A comparison (CT) between experimental and numerical results for Case 3

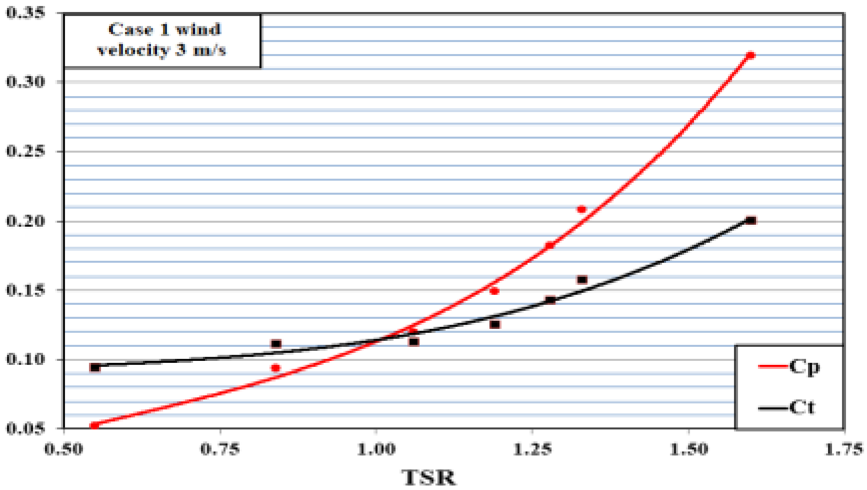

Figure 6.6-a: Performance parameters in terms of (Cp, CT) for Hybrid WT Case 1 (Experimental results)

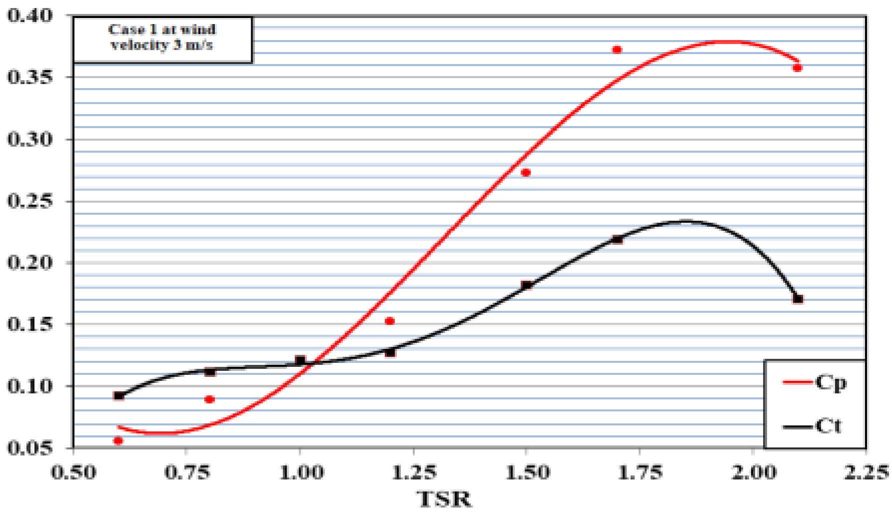

Figure 6.6-b: Performance parameters in terms of (Cp, CT) for hybrid WT Case 1 (Numerical results)

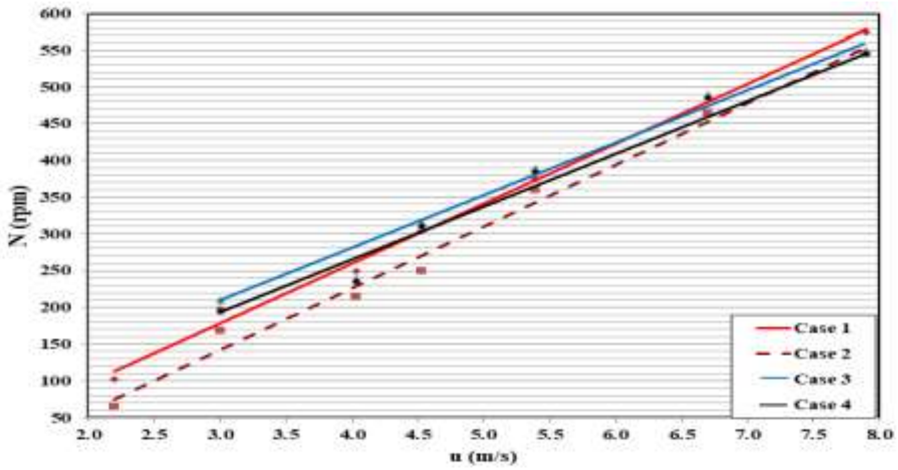

Figure 6.7-a: Relationship between the rotational speed (N) and wind velocity (u) (Experimental results)

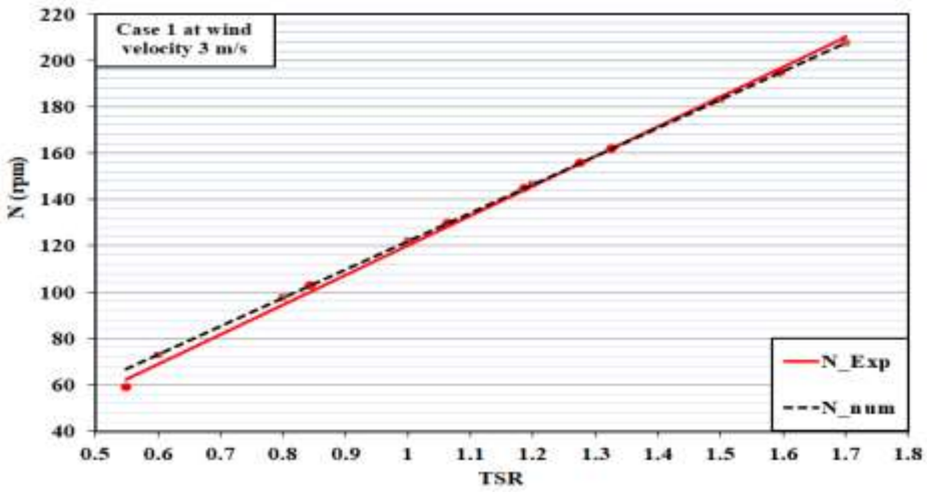

Figure 6.7-b: A comparison between experimental and numerical results for case 1 at constant wind velocity (3 m/s)

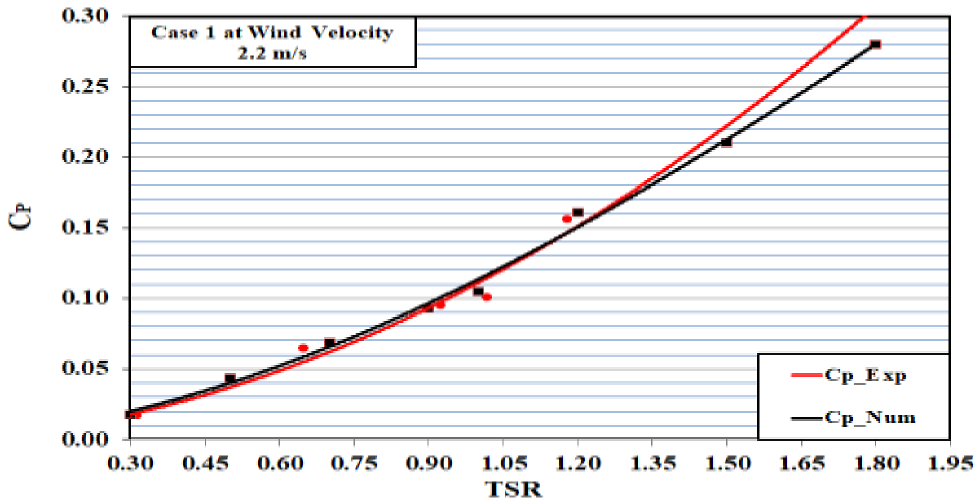

Figure 6.8-a: A comparison between experimental and numerical results: the relation between C_p and TSR for case 1 at wind velocity 2.2 m/s

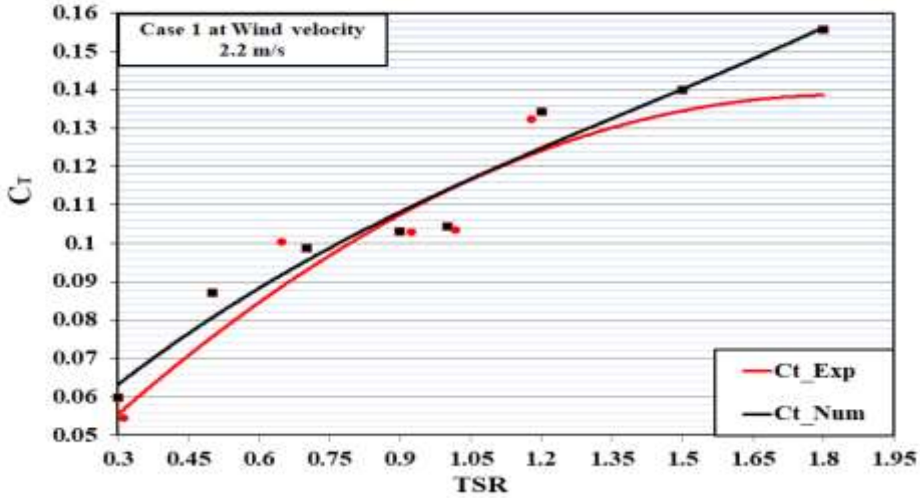

Figure 6.8-b: A comparison between experimental and numerical results:the relation between C_T and TSR for case 1 at wind velocity 2.2 m/s

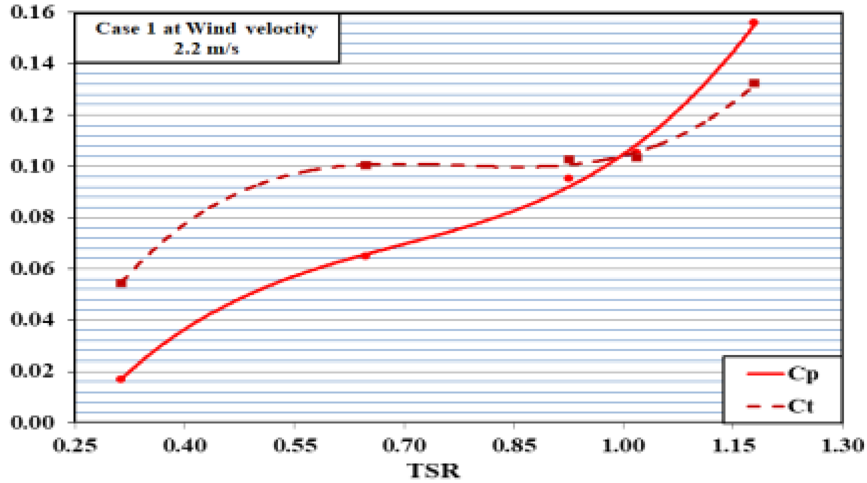

Figure 6.9-a: Performance parameters in terms of (C_P, C_T) for HWT case 1 at wind velocity 2.2 m/s (Experimental results)

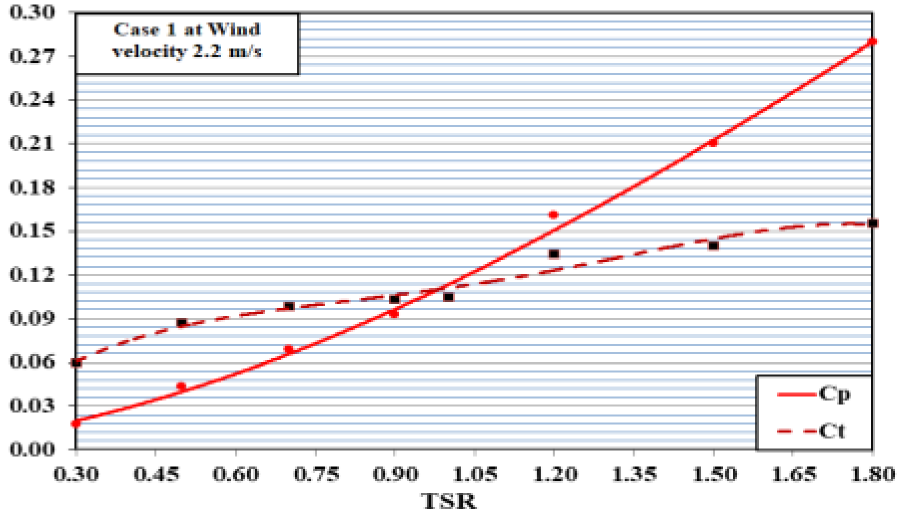

Figure 6.9-b: Performance parameters in terms of (C_P, C_T) for HWT case 1 at wind velocity 2.2 m/s (Numerical results)

REFERENCES

[1] https://energypedia.info/index.php?title=Assessing_Wind_Potentials&action=edit&mode=wysiwyg, "Wind Energy - Introduction".

[2] Biplab Kumar Debnath, Agnimitra Biswas and Rajat Gupta, Journal of Renewable and Sustainable Energy 1, 033110 (2009); doi: 10.1063/1.3152431 "Computational fluid dynamics analysis of a combined three-bucket Savonius and three bladed Darrieus rotor at various overlap conditions".

[3] Fang Feng, Shengmao Li, Yan Li, Dan Xu, Physics Procedia 24 (2012) 781 – 786, 2012 International Conference on Applied Physics and Industrial Engineering, "Torque characteristics simulation on small scale combined type vertical axis wind turbine".

[4] S.M. Rassoulinejad-Mousavi, M. Jamil and M. Layeghi, World Applied Sciences Journal 28(2): 205-211, 2013, ISSN1818-4952, 2013. "Experimental Study of a Combined Three Bucket H-Rotor with Savonius Wind Turbine".

[5] Xiaojing Sun, Yajun Chen, Yang Cao, GuoqingWu, Zhongquan Zheng and Diangui Huang., Advances in Mechanical Engineering 2016, Vol. 8(1) 1–11, The Author(s) 2016, aime.sagepub.com. "Research on the aerodynamic characteristics of a lift drag hybrid vertical axis wind turbine".

[6] Z. Anjum , L. A. Najmi , A. Fahad , R. Ashraf, S. Ehsan, W. Aslam ; Technical Journal, University of Engineering and Technology (UET) Taxila, Pakistan Vol. 21 No. IV-2016. "Common Vertical Axis Savonius-Darrieus Wind Turbines for Low Wind Speed Highway Applications".

[7] Ramesh K. Kavade and Pravin M. Ghanegaonkar, Journal of Clean Energy Technologies, Vol. 5, No. 5, September 2017, "Design and Analysis of Vertical Axis Wind Turbine for Household Application".

[8] Nawfal M. Ali, Sattar Aljabair, Abdul Hassan A.K., International Journal of Mechanical & Mechatronics Engineering IJMME-IJENS Vol:19 No:06, "An Experimental and Numerical Investigation on Darrieus Vertical Axis Wind Turbine Types at Low Wind Speed".

[9] Nawfal M. Ali, A.K. Abdul Hassan, Sattar Aljabair, Jour of Adv Research in Dynamical & Control Systems, Vol. 11, No. 11, 2019. "Effect of Conventional Multistage Savonius wind Turbines on the Performance of the Turbine at Low Wind Velocity".

[10] Mojtaba Tahani , Ali Rabbani, Alibakhsh Kasaeian, Mehdi Mehrpooya, Mojtaba Mirhosseini, Energy 130 (2017) 327-338, " Design and numerical investigation of Savonius wind turbine with discharge flow directing capability".

[11] M.H. Shojaeefard, M. Tahani, M.B. Ehghaghi, M.A. Fallahian, M. Beglari.(Computers & Fluids 60 (2012) 61–70). "Numerical study of the effects of some geometric characteristics of a centrifugal pump impeller that pumps a viscous fluid".

[12] K.K. Sharma, R. Gupta, A.Biswas , International Journal Of Renewable Energy Research, Vol.4, No.1, 2014. "Performance Measurement of a Two-Stage Two-Bladed Savonius Rotor".

[13] Frederikus Wenehenubuna, Andy Saputraa, Hadi Sutantoa, Energy Procedia 68 (2015) 297 – 304, 2nd International Conference on Sustainable Energy Engineering and Application, ICSEEA 2014 "An experimental study on the performance of Savonius wind turbines related with the number of blades".

[14] Argemiro Palencia Díaz, Giovanni Jiménez Pajaro, Khriscia Utria Salas, Ingeniare. Revista chilena de ingeniería, vol. 23 No 3, 2015, pp. 406-412, " Computational model of Savonius turbine".

[15] Jae-Hoon Lee, Young-Tae Lee, Hee-Chang Lim, Renewable Energy 89 (2016) 231-244, " Effect of twist angle on the performance of Savonius wind turbine".

[16] Mr. Laxmikant N.Dhoble1, Dr.A.K.Mahalle2, International Research Journal of Engineering and Technology (IRJET), Volume: 03 Issue: 01 | Jan-2016 "CFD Analysis Of Savonius Vertical Axis Wind Turbine: A Review".